Non-Sinusoidal Temporal Modulation in Circuits for Non-Reciprocity and Power Transfer

Juan Rafael Sánchez-Martínez*, Mario Pérez-Escribano†, Sergio Ortiz-Ruiz‡,
Juan F. Valenzuela-Valdés*, Pablo Padilla*, Carlos Molero*
Department of Signal Theory, Telematics and Communications, Research Centre for Information and Communication Technologies (CITIC-UGR), University of Granada, Granada, Spain
†Telecommunication Research Institute (TELMA), Universidad de Málaga,
E.T.S. Ingeniería de Telecomunicación, 29010 Málaga, Spain
‡Pervasive Electronics Advanced Research Laboratory, Department of Electronics and Computer Science,
Centre for Information, and Communication Technologies (CITIC-UGR) University of Granada, Granada, 18071, Spain
e-mail: cmoleroj@ugr.es

***Abstract*—In this paper, we demonstrate the improvement in circuit performance when time-varying circuits are modulated by non-sinusoidal waveforms. Specially we focus on triangular and rectangular modulations. By this, bandpass filters are designed and compared to conventional cases in order to exhibit the enhancement. Specially, the bandpass filters are desined to invoke non-reciprocity, an exotic and very interesting feature in time-modulated systems. A method of analysis based on the spectral domain is employed, establishing a general approach that is valid and applicable to other types of signals, as long as it is possible to obtain its decomposition in Fourier series. The results obtained from our model match those simulated using the Keysight ADS, thus validating the present approach.**

***Index Terms*—Band pass filter (BPF), non-reciprocal filters, resonators, spatiotemporal modulation (STM).**

I. Introduction

Reciprocity is a fundamental principle in electromagnetics, and applications involving microwave, millimeter, and photonics systems have benefited from it [1], [2]. Essentially, reciprocity implies that the field created by a source at an observation point is identical to the field when the positions of the observation point and the source are interchanged [3]. Classically typical components benefiting from reciprocal responses are filters [4], [5] and antennas [6], among others, where reciprocity is intended to improve spectral efficiencies by the reuse of the same channel for both transmitting and receiving signals.

In some contexts, otherwise, the demands on wireless communications require one-way propagation such as lasers or full-duplex communications [7]. Historically, non-reciprocal components have been designed and manufactured using magnetic materials or ferrites that exploit the Faraday effect to induce non-reciprocity [8]–[11]. Despite the good performance, the devices were large, bulky, and expensive, limiting their application in integrated circuits (IC). Lower-cost and lower-profile alternatives to break reciprocity were based on active devices, such as transistors [12]. But they typically have high noise figures and limited power-handling capacity, resulting in a moderate or low dynamic range [13].

To address these drawbacks, innovative approaches based on time modulation of circuit components have been proposed [14]. Time modulation has opened new opportunities for designing magnetic-free and low-profile non-reciprocal devices, with special emphasis on areas related to microwaves, photonics, and acoustics [15]–[18]. A remarkable advancement has been made in developing non-reciprocal band-pass filters (BPFs). The symmetry break in BPFs combines isolation and filtering functions into a single device [19], [20]. These devices, known as *isolating filters*, employ topologies based on cascades of time-modulated coupled resonators. The resonators are essentially shunt connections between regular inductors and periodically time-varying capacitors, whose modulation is usually sinusoidal [21], [22]. Reducing the complexity in both the theoretical calculations and the experimental part inspires the analysis of sinusoidally time-modulated capacitors.

The exploration of non-sinusoidal modulations in capacitors and their implications in BPFs have never been implemented nor proposed to the authors' knowledge. Theoretical analysis has indeed been detailed for general periodic modulation based on circuit approaches in contexts such as metasurfaces [23], [24]. In any case, they have never been particularized for triangular or rectangular modulations. This paper explores the performance of BPFs based on cascades of non-sinusoidally time-modulated resonators. As will be shown, triangular or rectangular modulations can improve key characteristics of non-reciprocal BPFs with sinusoidal modulation, such as low-forward transmission losses, high reverse isolation, and directivity. These modulations also add robustness to the circuits in some critical scenarios. Moreover, understanding how different modulation techniques affect these devices' performance is crucial for comprehending their operation and optimizing non-reciprocity at the carrier frequency under various operating conditions.

II. Analysis of Time-Varying Circuits

The analysis of linear time-varying (LTV) circuits with time-harmonic variation focuses on studying circuits where

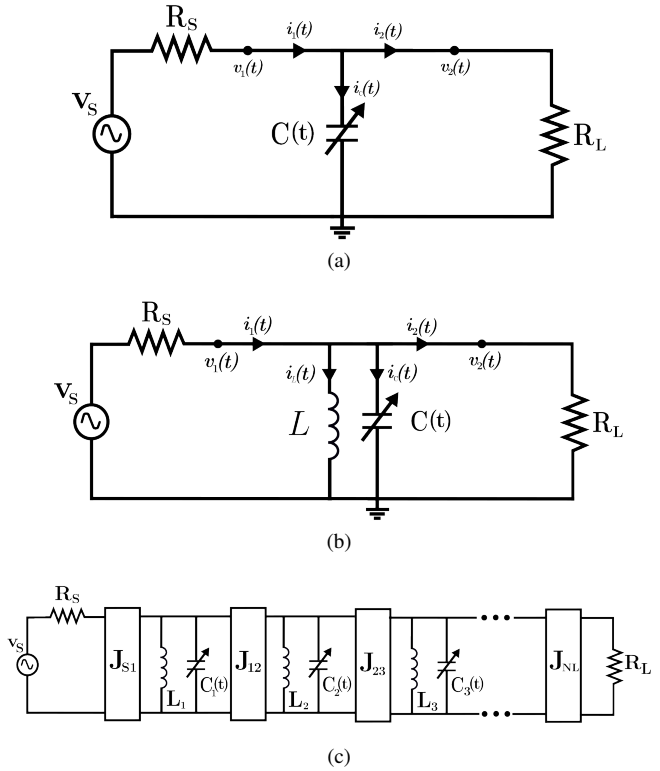

Fig. 1. (a) Simple LTV circuit with a parallel capacitor modulated by a single sinusoidal. (b) LC resonator in parallel incorporating a time-invariant inductor L and a time-varying capacitor $C(t)$. (c) Topology of the space-time modulated filter of order n.

any of the components varies periodically with time. When the circuit is excited by a different frequency ω (henceforth called carrier frequency) compared to that modulating the circuit component ω_m, the global response of the system in terms of voltage and current are periodic signals that admit to be described by an infinite summation of harmonics. Each of the harmonics has its own frequency $\omega + i\omega_m$ resulting from the intermodulation products (IM) with $i \in Z$. The main concern consists of evaluating the amplitude of these harmonics, which subsequently gives rise to the evaluation of the whole voltage and current.

Let us first consider an elementary LTV circuit consisting of a single time-varying shunt capacitor, $C(t)$, as shown in Fig. 1a. The time-varying capacitor is connected to a voltage source V_s with internal resistance R_s. Thanks to the periodicity of the problem, the analysis of this circuit can be accounted for by the spectral domain method [25]. After a few calculations, the relationship between the voltages and currents at both ports can be expressed in the frequency domain in the form of the next generalized ABCD matrix [26]

$$\begin{pmatrix} \mathbf{V}_1 \\ \mathbf{I}_1 \end{pmatrix} = \begin{pmatrix} \hat{\mathbf{U}} & \hat{\mathbf{0}} \\ \hat{\mathbf{Y}}_\mathrm{C} & \hat{\mathbf{U}} \end{pmatrix} \begin{pmatrix} \mathbf{V}_2 \\ \mathbf{I}_2 \end{pmatrix}, \tag{1}$$

where $\mathbf{V}_{1/2}$ and $\mathbf{I}_{1/2}$ are vectors whose entries are the individual voltages associated with each of the harmonics. For example, $\mathbf{V}_1$ is expressed as

$$\mathbf{V}_1 = [..., v_{-p}^{(1)}, ..., v_1^{(1)}, ...v_p^{(1)}, ...], \tag{2}$$

where $v_p^{(1)}$ is the voltage related to the pth-harmonic. $\hat{\mathbf{U}}$ is the identity matrix and $\hat{\mathbf{0}}$ is the zero matrix.

Special mention deserves the spectral admittance matrix $\hat{\mathbf{Y}}_\mathrm{C}$, which directly depends on the modulation. Assuming a capacitor periodically modulated in the following form

$$C(t) = C_0 + \Delta C f(t), \tag{3}$$

being $f(t)$ a periodic function, and $C_0 > \Delta C f(t)\ \forall t$, $\hat{\mathbf{Y}}_\mathrm{c}$ is mathematically expressed as in (4). The diagonal elements correspond to the admittance at each IM frequency, and the off-diagonal elements correspond to the transconductance between different intermodulation frequencies (modulated terms). The parameter ξ is the denominated modulation ratio, defined as $\xi = \Delta C/C_0$. Otherwise, K_n are related to the Fourier-transform coefficients of the modulation signal. Finally, the phase factor ϕ represents the modulating signal's phase-shift with respect to the carrier signal. The resulting matrix is a generalization of that in [19], where they consider a sinusoidal modulation (see Fig. 2a) controlling the time variation of the capacitor. Under the sinusoidal modulation (4) reduces to a matrix where $K_0 = C_0$, $K_1 = K_{-1} = c_1/2$ and $K_n = 0$ for $n \neq 0, \pm 1$. This paper extends the analysis to different periodic modulations controlling the capacitor evolution. We especially remark on the triangular- and rectangular-modulations shapes. Fig. 2b and Fig. 2c illustrates them, that logically lead to different values for K_n in each case. The extension of the analysis to time-varying resonators [27] is shown in Fig. 1b. The main difference from the previous case is the presence of a regular inductor connected parallel to the time-varying capacitor. This constitutes a unit block. A cascade of several unit blocks results in the BPF configuration shown in Fig. 1c. The BPF comprises the fundamental blocks of many spatial and temporal modulation (STM) circuits. A key element for the design of these multi-stage resonators is the admittance inverters [28], which are conveniently tuned to provide full matching between the different blocks. The general ABCD matrix of a single resonator is now defined as

$$\hat{\mathbf{Y}}_\mathrm{C} = j \begin{bmatrix} \ddots & \vdots & \vdots & \vdots & \vdots & \vdots & \iddots \\ \cdots & (\omega - 2\omega_m)K_0 & (\omega - 2\omega_m)K_1 e^{-j\phi} & (\omega - 2\omega_m)K_2 e^{-j\phi} & (\omega - 2\omega_m)K_3 e^{-j\phi} & (\omega - 2\omega_m)K_4 e^{-j\phi} & \cdots \\ \cdots & (\omega - \omega_m)K_{-1} e^{j\phi} & (\omega - \omega_m)K_0 & (\omega - \omega_m)K_1 e^{-j\phi} & (\omega - \omega_m)K_2 e^{-j\phi} & (\omega - \omega_m)K_3 e^{-j\phi} & \cdots \\ \cdots & \omega K_{-2} e^{j\phi} & \omega K_{-1} e^{j\phi} & \omega K_0 & \omega K_1 e^{-j\phi} & \omega K_2 e^{-j\phi} & \cdots \\ \cdots & (\omega + \omega_m)K_{-3} e^{j\phi} & (\omega + \omega_m)K_{-2} e^{j\phi} & (\omega + \omega_m)K_{-1} e^{j\phi} & (\omega + \omega_m)K_0 & (\omega + \omega_m)K_1 e^{-j\phi} & \cdots \\ \cdots & (\omega + 2\omega_m)K_{-4} e^{j\phi} & (\omega + 2\omega_m)K_{-3} e^{j\phi} & (\omega + 2\omega_m)K_{-2} e^{j\phi} & (\omega + 2\omega_m)K_{-1} e^{j\phi} & (\omega + 2\omega_m)K_0 & \cdots \\ \iddots & \vdots & \vdots & \vdots & \vdots & \vdots & \ddots \end{bmatrix}, \tag{4}$$

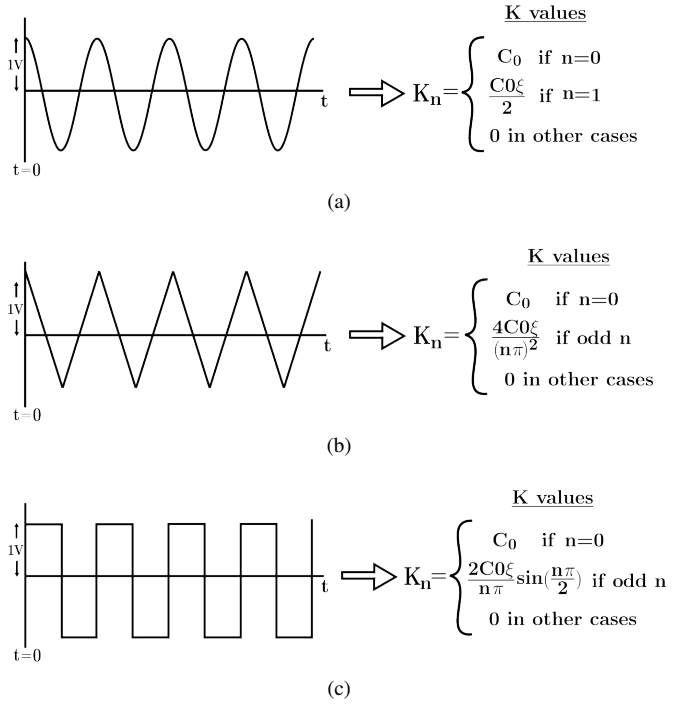

Fig. 2. Values of the K_n constants in the complex admittance matrix of the capacitor for different waveforms: (a) Sinusoidal, (b) Triangular, (c) rectangular.

$$\hat{\mathbf{N}}_{\mathrm{LC}} = \begin{pmatrix} \hat{\mathbf{U}} & \hat{\mathbf{0}} \\ \hat{\mathbf{Y}}_{\mathrm{LC}} & \hat{\mathbf{U}} \end{pmatrix} = \begin{pmatrix} \hat{\mathbf{U}} & \hat{\mathbf{0}} \\ \hat{\mathbf{Y}}_{\mathrm{C}} + \hat{\mathbf{Y}}_{\mathrm{L}} & \hat{\mathbf{U}}, \end{pmatrix} \tag{5}$$

with $\hat{\mathbf{Y}}_{\mathrm{L}}$ being a diagonal matrix associated with the inductor

$$\hat{\mathbf{Y}}_{\mathrm{L}} = -\mathrm{j}(L_0)^{-1} \begin{bmatrix} \ddots & \vdots & \vdots & \vdots & \iddots \\ \cdots & (\omega-\omega_m)^{-1} & 0 & 0 & \cdots \\ \cdots & 0 & \omega^{-1} & 0 & \cdots \\ \cdots & 0 & 0 & (\omega+\omega_m)^{-1} & \cdots \\ \iddots & \vdots & \vdots & \vdots & \ddots \end{bmatrix}, \tag{6}$$

Furthermore, the ABCD-formalism is adequate to easily get the matrix form for the whole BPF. For instance, for a BPF with 3 unit blocks, we can write the resulting matrix just by applying the matrix product between all the circuit elements:

$$\hat{\mathbf{N}}_3 = \hat{\mathbf{N}}_{\mathrm{JS1}}\hat{\mathbf{N}}_{\mathrm{LC1}}\hat{\mathbf{N}}_{\mathrm{J12}}\hat{\mathbf{N}}_{\mathrm{LC2}}\hat{\mathbf{N}}_{\mathrm{J23}}\hat{\mathbf{N}}_{\mathrm{LC3}}\hat{\mathbf{N}}_{\mathrm{J3L}}, \tag{7}$$

where the matrices $\hat{\mathbf{N}}_{\mathrm{J}\alpha}$ represent the matrix of the inverters

$$\mathbf{N}_{\mathrm{J}\alpha} = \begin{pmatrix} \hat{\mathbf{0}} & \pm\mathrm{j}\hat{\mathbf{J}_\alpha}^{-1} \\ \mp\mathrm{j}\hat{\mathbf{J}_\alpha} & \hat{\mathbf{0}} \end{pmatrix} \tag{8}$$

with α being S1 (inverter from source to resonator 1), 12 (inverter from resonator 1 to resonator 2), and so on. Once the complete ABCD matrix $\hat{\mathbf{N}}_3$ is computed the calculation of the S-parameters becomes relatively straightforward [19], [26].

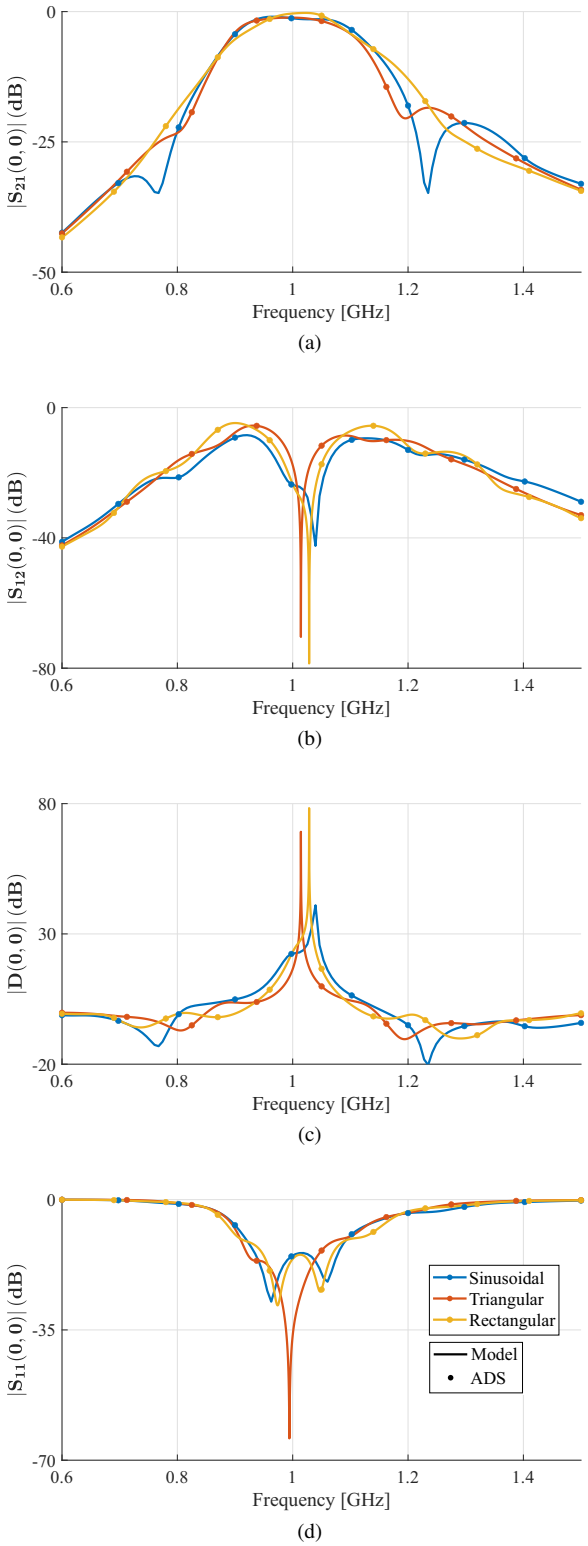

Fig. 3. S-parameters of the three-stage filter. Circuit values: $J_{S1} = J_{3L} = 0.0119\Omega^{-1}$, $J_{12} = J_{23} = 0.0062\Omega^{-1}$, $R_S = R_L = 50\Omega$, $L_0 = 4nH$, and a static capacitor value of $C_0 = 6.37pF$. The results include: (a) $|S21,(0,0)|$, (b) $|S12,(0,0)|$ (c) $D(0,0)$, and (d) $|S11,(0,0)|$.

III. Results

This section explores a three-stage BPF when triangular and rectangular periodic forms control the capacitor. We will

demonstrate that the structure is non-reciprocal even with these new modulations. That is, when the carrier signal enters from one side of the circuit, the circuit's response will be different than in the case of the carrier signal entering from the opposite side. In mathematical language, $S_{21}(0,0) \neq S_{12}(0,0)$, with (0, 0) referring to the carrier mode. To quantify the non-reciprocity, 2 additional parameters are defined: directivity $D(0,0)$, denoting the difference in power between $S_{21}(0,0)$ and $S_{12}(0,0)$ of the carrier mode; and reverse isolation $S_{11}(0,0)$. The design specifications for this three-stage BPF will be centered on a frequency of 1 GHz and a 3 dB-passband of about 230 MHz. It is worth noting that thanks to the model, parametric studies in terms of the modulation parameters (ω_m, ξ, and ϕ) are very fast. The parametric study allows us to identify the optimal values maximizing filter performance. The three waveforms in Fig. 2 have been employed for the parametric study. The resulting optimal parameters are:

- Sinusoidal: $\omega_m = 2\pi \cdot 150 \cdot 10^6 s^{-1}$, $\xi = 0.27$ and $\phi = 45^o$.
- Triangular: $\omega_m = 2\pi \cdot 105 \cdot 10^6 s^{-1}$, $\xi = 0.26$ and $\phi = 50^o$.
- Rectangular: $\omega_m = 2\pi \cdot 150 \cdot 10^6 s^{-1}$, $\xi = 0.19$ and $\phi = 85^o$.

The corresponding results are plotted in Fig. 3. For the sinusoidal modulation, the filter exhibits a minimum insertion loss $[-S_{21}(0,0)]$ of 1.3 dB, a return loss $[-S_{11}(0,0)]$ greater than 14 dB, and reverse isolation $[-S_{12}(0,0)]$ reaching 42 dB, resulting in a directivity $[D(0,0)]$ close to 41 dB. The triangular slight modulation improves the insertion loss, reaching a minimum of 1.1 dB. However, the return loss is excellent, with values close to 60 dB and the reverse isolation reaching 70 dB. The directivity now goes up to around 69 dB. Finally, the rectangular waveform offers the best performance, achieving a minimum insertion loss of approximately 0.2 dB, a return loss greater than 16 dB, and reverse isolation of 78.5 dB, which translates to a directivity of 78.25 dB. The results have been compared to those provided by the commercial software ADS. In ADS, it is possible to solve this kind of circuit using the Harmonic-Balance simulation. The agreement between the commercial software and the model reported here is very good.

It is worth mentioning that the triangular and rectangular modulations are less sensitive to slight variations of the parameters. In the case of sinusoidal modulation, it is not possible to improve the insertion losses without provoking a deterioration in the directivity, and vice versa. The rectangular waveform, otherwise, is much less sensitive to this since the degrees of freedom have increased. It is, therefore, possible to enhance insertion losses without degrading the directivity. Thus, another type of modulation, such as the rectangular one, provides robustness to the circuit performance, especially in scenarios when fine-tuning is critical.

IV. Design and Real Implementation

In this section, the design and implementation of a prototype filter consisting of a single resonator stage will be carried out, formed by a regular inductor and a time-varying capacitor. A single-stage filter is first proposed to advance towards the three-stage one. After a few simulations in ADS, the values of the components selected for the design are as follows: input and output port resistances of 50Ω, a nominal or static capacitance of 0.6 nF, a static inductor of 2.2 nH, and a varactor diode SMV1234 that acts as a variable capacitance [29]. Additionally, the different traces of the circuit are transmission lines (TL) adapted to 50Ω. Figure 4 shows the manufactured circuit. Since the fabrication of this prototype is recent, it is conceived to be experimentally tested in the following weeks, as well as the proposal, design, fabrication, and experimental validation of the three-stage filter.

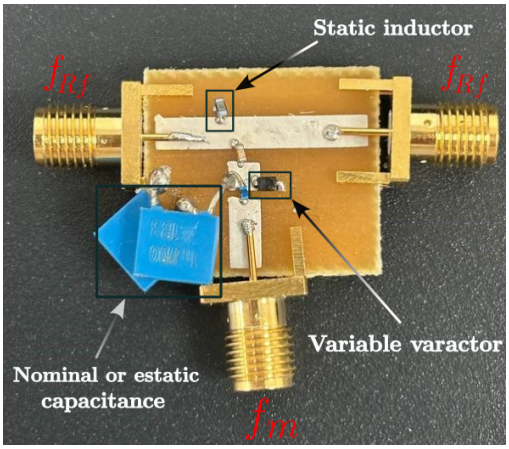

Fig. 4. Implementation of the circuit manufactured with a single resonator stage.

V. Conclusion

In this paper, we have demonstrated how the modulation of the resonators, using non-sinusoidal waveforms such as triangular and rectangular modulation, can significantly improve the performance of a non-reciprocal bandpass filter compared to traditional sinusoidal modulations. The analysis, based on the expansion of time-varying capacitance in Fourier series, has allowed us to establish a general approach applicable to different types of signals, providing a deeper understanding of how modulation techniques influence the transmission and isolation characteristics of the filter. The results from simulations in ADS and the analytical model confirm the non-reciprocal behavior of the filter, highlighting its viability for simultaneous transmission and reception of broadband signals. This study broadens the design of non-reciprocal filters and suggests that new modulation forms could open opportunities for advanced communications and signal processing technologies.

Acknowledgment

This work has been supported by grant TED2021-129938B-I00 funded by MCIN/AEI/10.13039/501100011033 and by the European Union NextGenerationEU/PRTR. It has also been supported by grants PID2020-112545RBC54, PDC2022-133900-I00, PDC2023-145862-I00, and IJC2020-043599-I, funded by MCIN/AEI/10.13039/501100011033 and by the European Union NextGenerationEU/PRTR.

REFERENCES

[1] J. D. Jackson, *Classical electrodynamics*. John Wiley & Sons Inc, 1998.

[2] R. E. Collins, *Field Theory of Guided Waves*. Wiley IEEE Press, 1991.

[3] V. Asadchy, M. S. Mirmoosa, A. Díaz-Rubio, S. Fan, and S. Tretyakov, "Tutorial on electromagnetic nonreciprocity and its origins," 01 2020.

[4] V. C. Benjin, *Advance in multi-band microstrip filters*. Cambridge University Press, 2015.

[5] A. Fernández-Prieto, A. Lujambio, J. Martel, F. Medina, F. Mesa, and R. R. Boix, "Simple and compact balanced bandpass filters based on magnetically coupled resonators," *IEEE Transactions on Microwave Theory and Techniques*, vol. 63, no. 6, pp. 1843–1853, 2015.

[6] C. A. Balanis, *Antenna Theory - Analysis and design*. John Wiley & Sons, 2005.

[7] D. Bharadia, E. McMilin, and S. Katti, "Full duplex radios," in *Proceedings of the ACM SIGCOMM 2013 Conference on SIGCOMM*, ser. SIGCOMM '13. New York, NY, USA: Association for Computing Machinery, 2013, p. 375–386. [Online]. Available: https://doi.org/10.1145/2486001.2486033

[8] C. Fay and R. Comstock, "Operation of the ferrite junction circulator," *Microwave Theory and Techniques, IEEE Transactions on*, vol. MTT-13, pp. 15 – 27, 02 1965.

[9] C. Seewald and J. Bray, "Ferrite-filled antisymmetrically biased rectangular waveguide isolator using magnetostatic surface wave modes," *Microwave Theory and Techniques, IEEE Transactions on*, vol. 58, pp. 1493 – 1501, 07 2010.

[10] D. Taft, G. Jr, and H. Jr, "Millimeter resonance isolators utilizing hexagonal ferrites," *Microwave Theory and Techniques, IEEE Transactions on*, vol. 11, pp. 346 – 356, 10 1963.

[11] Y. Konishi, "Lumped element circulators," *Magnetics, IEEE Transactions on*, vol. 11, pp. 1262 – 1266, 10 1975.

[12] S. Taravati and G. V. Eleftheriades, "Transistor-loaded nonmagnetic nonreciprocal metasurfaces," in *2021 International Applied Computational Electromagnetics Society Symposium (ACES)*, 2021, pp. 1–4.

[13] G. Carchon and B. Nanwelaers, "Power and noise limitations of active circulators," *Microwave Theory and Techniques, IEEE Transactions on*, vol. 48, pp. 316 – 319, 03 2000.

[14] C. Caloz, A. Alù, S. Tretyakov, D. Sounas, K. Achouri, and Z.-L. Deck-Léger, "Electromagnetic nonreciprocity," *Phys. Rev. Appl.*, vol. 10, p. 047001, Oct 2018. [Online]. Available: https://link.aps.org/doi/10.1103/PhysRevApplied.10.047001

[15] Z. Yu and S. Fan, "Complete optical isolation created by indirect interband photonic transitions," *Nature Photonics*, vol. 3, 02 2009.

[16] H. Lira, Z. Yu, S. Fan, and M. Lipson, "Electrically driven nonreciprocity induced by interband photonic transition on a silicon chip," *Physical review letters*, vol. 109, p. 033901, 07 2012.

[17] D. Correas Serrano, J. Gomez-Diaz, D. Sounas, Y. Hadad, A. Melcón, and A. Alu, "Non-reciprocal graphene devices and antennas based on spatio-temporal modulation," *IEEE Antennas and Wireless Propagation Letters*, vol. 15, pp. 1–1, 01 2015.

[18] S. Qin, Q. Xu, and E. Wang, "Nonreciprocal components with distributedly modulated capacitors," *Microwave Theory and Techniques, IEEE Transactions on*, vol. 62, pp. 2260–2272, 10 2014.

[19] X. Wu, X. Liu, M. D. Hickle, D. Peroulis, J. S. Gómez-Díaz, and A. Álvarez Melcón, "Isolating bandpass filters using time-modulated resonators," *IEEE Transactions on Microwave Theory and Techniques*, vol. 67, no. 6, pp. 2331–2345, 2019.

[20] X. Wu, M. Nafe, A. A. Melcón, J. Sebastián Gómez-Díaz, and X. Liu, "A non-reciprocal microstrip bandpass filter based on spatio-temporal modulation," in *2019 IEEE MTT-S International Microwave Symposium (IMS)*, 2019, pp. 9–12.

[21] G. Chaudhary and Y. Jeong, "Rigorous design and experimental validation of non-reciprocal bandpass filter with ultrawide high reverse isolation bandwidth," *Engineering Science and Technology, an International Journal*, vol. 52, p. 101674, 2024. [Online]. Available: https://www.sciencedirect.com/science/article/pii/S2215098624000600

[22] Y. Jiao and X. Wang, "A non-reciprocal lc filter structure and its design methodology," *Journal of Physics: Conference Series*, vol. 2810, no. 1, p. 012013, jul 2024. [Online]. Available: https://dx.doi.org/10.1088/1742-6596/2810/1/012013

[23] X. Wang, A. Díaz-Rubio, H. Li, S. A. Tretyakov, and A. Alù, "Theory and design of multifunctional space-time metasurfaces," *Phys. Rev. Appl.*, vol. 13, p. 044040, Apr 2020. [Online]. Available: https://link.aps.org/doi/10.1103/PhysRevApplied.13.044040

[24] G. Ptitcyn, M. S. Mirmoosa, A. Sotoodehfar, and S. A. Tretyakov, "A tutorial on the basics of time-varying electromagnetic systems and circuits: Historic overview and basic concepts of time-modulation," *IEEE Antennas and Propagation Magazine*, vol. 65, no. 4, pp. 10–20, 2023.

[25] C. Kurth, "Steady-state analysis of sinusoidal time-variant networks applied to equivalent circuits for transmission networks," *IEEE Transactions on Circuits and Systems*, vol. CS-24, no. 11, pp. 610–624, Nov 1977.

[26] D. M. Pozar, *Electromagnetic theory in microwave engineering*. John Wiley & Sons Inc, 2005.

[27] R. Lu, T. Manzaneque, A. Gao, L. Gao, and S. Gong, "A radio frequency non-reciprocal network based on switched low-loss acoustic delay lines," 05 2018, pp. 102–104.

[28] M. Steer, *Microwave and RF Design IV: Modules*. North Carolina State University, 2024.

[29] Skyworks Solutions, Inc., "Smv1234-079lf: Hyperabrupt junction tuning varactor diode," 2024, accessed: 2024-06-22. [Online]. Available: https://pdf1.alldatasheet.com/datasheet-pdf/view/155315/SKYWORKS/SMV1234-079LF.html